Supplementary Information

Methyl Regulation Triggers High-Temperature Ferroelastic Phase Transition

Si-Yue Zhang[a], Zhi-Cheng Zhang[a], Tie Zhang[a], Hao-Fei Ni[b], Zhi-Xu Zhang[b], Da-Wei Fu[a]* and Hai-Feng Lu[b]*

[a.] Ordered Matter Science Research Center, Jiangsu Key Laboratory for Science and Applications of Molecular Ferroelectrics, Southeast University, Nanjing 211189, People's Republic of China. (E-mail: dawei@seu.edu.cn, zhixu@seu.edu.cn)

[b.] Institute for Science and Applications of Molecular Ferroelectrics, Key Laboratory of the Ministry of Education for Advanced Catalysis Materials, Zhejiang Normal University, Jinhua, 321004, People's Republic of China. (E-mail: luhaifeng@zjnu.edu.cn)

EXPERIMENTAL

Materials. Tetramethyl ammonium iodide (Macklin, AR 98%), Trimethylamine solution (Aladdin, 30 wt. % in H_2O), Bromoethane (Macklin, AR 98%), Trimethylpropylammonium Bromide (Macklin, ≥98%), 2-Bromopropane (Aladdin, ≥99.8%), Hydroiodic acid (Macklin, AR ≥47.0%), Cadmium iodide (Macklin, AR 99.5%) were used as received without further purification, Acetonitrile(Aladdin, AR, >99%).

Synthesis of TMEABr. Place a round bottom flask containing 100 mmol trimethylamine and 100 mmol bromoethane on a thermostatic magnetic stirring device, then add ethanol as solvents and stir at 313 K for 24 h. After the end of the reaction, vacuum distillation is carried out at 333 K until it stops when no liquid is distilled. Trimethyl ethyl bromide (TMEABr) was obtained by using acetone washing products.[1] The specific test structure data and elemental analysis test data are placed in the attachment (Table S1).

Synthesis of TMIPABr. Add 100 mmol of trimethylamine and 100 mmol of 2-Bromopropane to a round bottom flask, then add acetonitrile and stir at 308 K for 24 h. Solvent-free crystals trimethylisopropylammonium bromide (TMIPABr) were then obtained by rotary evaporation at 60 °C.[2]

Synthesis of $[TTMA]_2CdI_4$, $[TMEA]_2CdI_4$, $[TMIPA]_2CdI_4$ and $[TMPA]_2CdI_4$. $[TTMA]_2CdI_4$, $[TMEA]_2CdI_4$, $[TMIPA]_2CdI_4$ and $[TMPA]_2CdI_4$ single crystals were prepared by slow evaporation of HI solutions containing 2:1 mmol amounts of organic ammonium salts and CdI_2. Dissolve 4 mmol organic ammonium salts in 10 mL aqueous solution and sequentially add to 10 mL HI solution containing 2 mmol CdI_2. Stir the mixture for 30 min and evaporate slowly at 40 °C. After three days, single crystals precipitated out of the solution.

EXPERIMENTAL MEASUREMENT METHODS

Differential Scanning Calorimetry (DSC). DSC measurements of compounds were characterized using a NETZSCH-214 instrument, and microcrystalline compounds were heated and cooled in an aluminum crucible with the rate of 20 K/min.

Single-Crystal X-ray Diffraction (SXRD). The crystallographic structures of compounds were identified by using a Rigaku single-crystal X-ray diffractometer with Mo-Kα radiation (λ = 0.71073 Å). The structures of samples were determined by direct methods and refined by the full matrix method through the SHELXTL software package. All non-hydrogen atoms were refined anisotropically, and all hydrogen atoms which were generated geometrically possessed isotropic displacement parameters. Detailed crystal data and refinement parameters are shown in Table S1. Moreover, the crystallographic structures of compounds have been deposited at the Cambridge Crystallographic Data Center (CCDC) (deposition numbers: 2254166, 2254168-2254171 and 2260835-2260836) and can be obtained free of charge from

the CCDC *via* www.ccdc.cam.ac.uk/getstructures.

Powder X-ray Diffraction (PXRD). The powder X-ray diffraction patterns of microcrystalline compounds were characterized by using a Rigaku D-MAX diffraction system using Cu-kα radiation in the 2θ range from 5° to 55° with a step size of 0.02° at 298 K. Simulated powder patterns of samples were calculated by Mercury software package using the crystallographic information file from the single-crystal X-ray experiment.

Hirshfeld surfaces analysis. Hirschfeld surfaces and associated 2D-fingerprint plots are calculated by entering CIF structure files into CrystalExplorer program. Hirshfeld surfaces of three compounds were obtained using a standard (high) surface resolution, which can provide the information about intermolecular interactions in the crystal. The 2D fingerprint plot is a combination of d_e and d_i that provides the summary of intermolecular contacts in the crystal and is in complement to the Hirshfeld surfaces, where d_i is the distance to the nearest atom center interior to the surface, and d_e exterior to the surface. The normalized contact distance d_{norm} is calculated according to d_e, d_i, the van der Waals (vdW) radii of the two atoms external (r_e^{vdW}) and internal (r_i^{vdW}) to the surface:

$$d_{\text{norm}} = \frac{d_i - r^{vdW}}{r_i^{vdW}} - \frac{d_e - r}{r_e^{vdW}}$$

d_{norm} surface is used for the identification of close intermolecular interactions. The value *dnorm* is negative or positive when intermolecular contacts are shorter or longer than r^{vdW}, respectively. Hirshfeld surface with dnorm values display a red-blue-white color scheme: where red regions correspond to closer contacts and negative d_{norm} value; the blue regions correspond to longer contacts and positive d_{norm} value; and the white regions correspond to the distance of contacts is exactly the van der Waals separation and with a d_{norm} value of zero.

Ferroelastic Measurement. For the observation of ferroelastic domain, 20 mg of dried powder of 3 was dissolved in 2 ml of a 1:1 mixture of water and DMF, dissolving completely to form a precursor solution. Specifically, 20 μL of precursor solution was spread on a clean ITO (indium tin oxide) glass which underwent the surface treatment by an S-3 ozone instrument, and then annealed at 323 K for 30 min. The domain structure was observed by using an Olympus BX51TRF polarizing microscope with a variable temperature system, where the temperature control system was the INSTEC HCC602 cooling/heating stage. During the heating and cooling cycles, the evolution of the ferroelastic domain structure was observed for **3**.

Dielectric Measurements. For dielectric characterization, these crystals were ground into powder with a mortar and pestle, and the appropriate quantity of powder is pressed into a thin sheet with a thickness of about 4 mm. The flakes were glued to the electrodes through conductive silver glue and copper wire to make capacitors for dielectric measurements. In the temperature range of 248-405 K, the complex dielectric constant ε is measured by the TH2828A instrument. The complex dielectric permittivity ε ($\varepsilon = \varepsilon' - i\varepsilon''$), where ε' is the real part, and ε'' is the imaginary part, dielectric loss $\tan\delta = \frac{\varepsilon''}{\varepsilon'}$

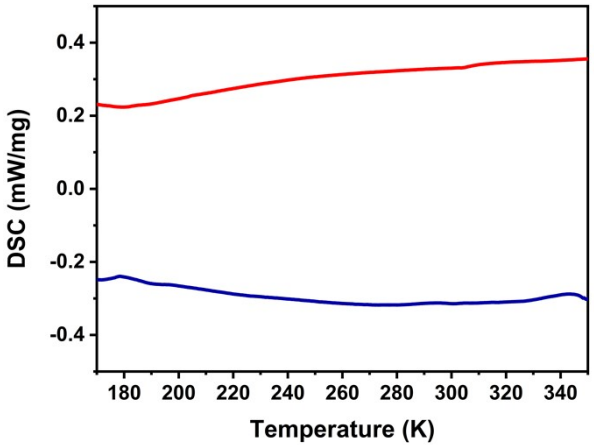

Fig. S1 DSC curves of **4** in heating-cooling cycle.

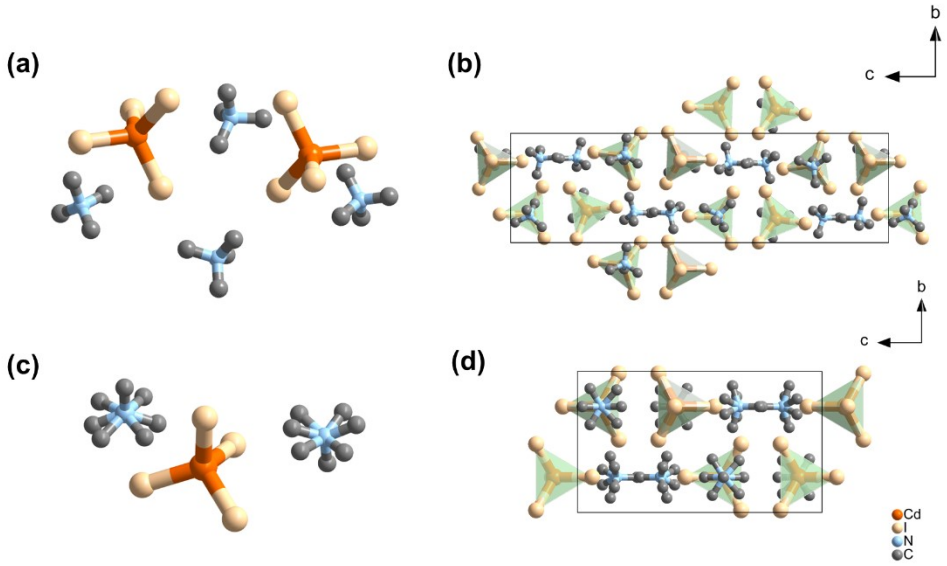

Fig. S2 (a) Molecular structure of **1** at LTP_1. (b) Unit cell packing view of compound **1** along a-axis at LTP_1. (c) Molecular structure of **1** at HTP_1. (d) Unit cell packing view of compound **1** along a-axis at HTP_1. H atoms has been omitted to make the structure clearer.

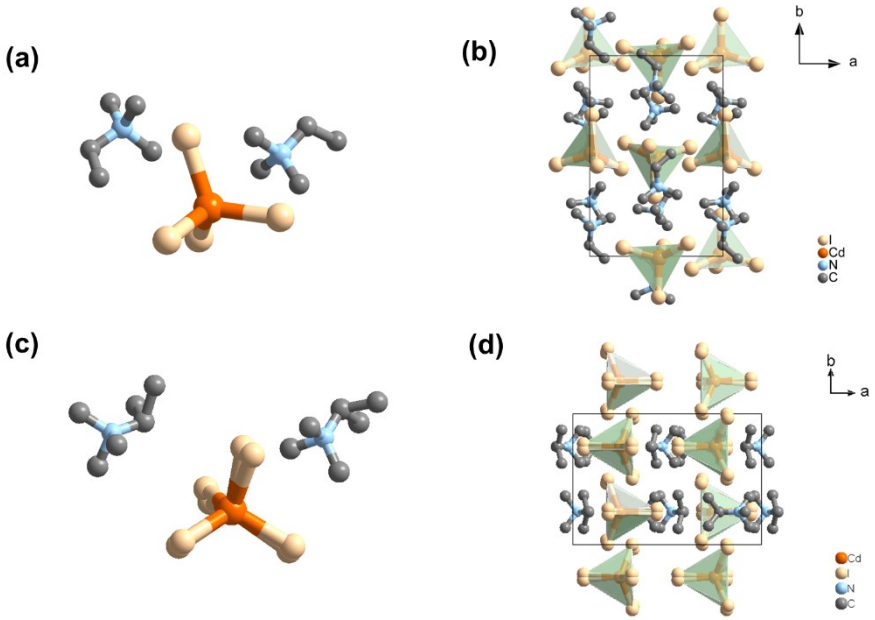

Fig. S3 (a) Molecular structure of **2** at LTP_2. (b) Unit cell packing view of compound **2** along c-axis at LTP_2. (c) Molecular structure of **2** at HTP_2. (d) Unit cell packing view of compound **2** along c-axis at HTP_2. H atoms has been omitted to make the

structure clearer.

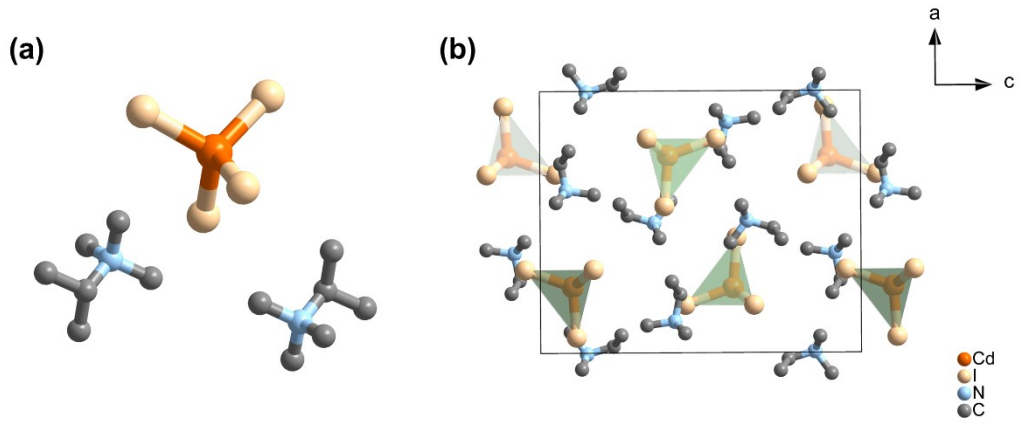

Fig. S4 (a) Molecular structure of compound **4**. (b) Unit cell packing view of compound **4** along b axis. H atoms has been omitted to make the structure clearer.

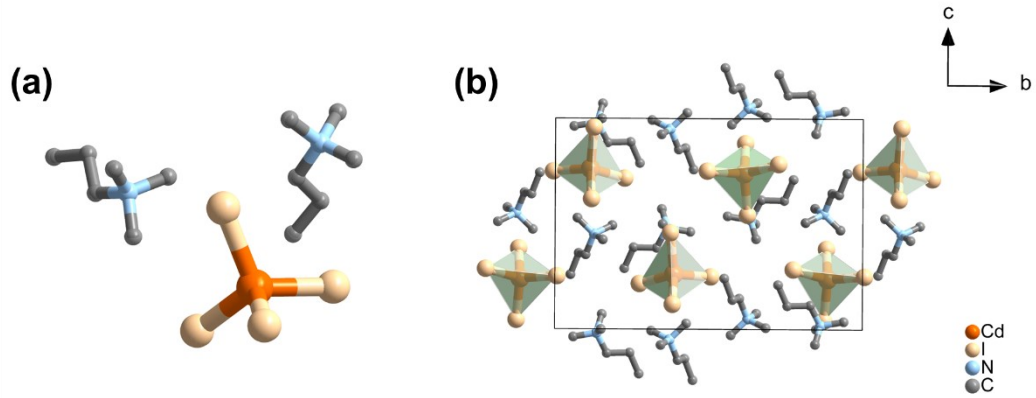

Fig. S5 (a) Molecular structure of compound **3** at LTP_3. (b) Unit cell packing view of compound **3** along a axis at LTP_3. H atoms has been omitted to make the structure clearer.

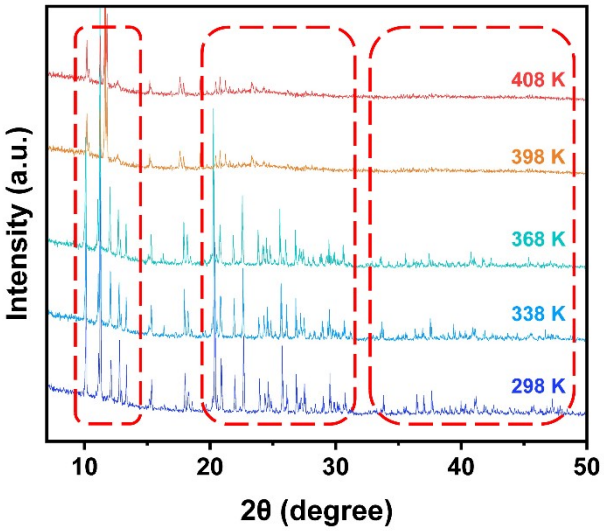

Fig. S6 VT-PXRD curves of Compound **3**.

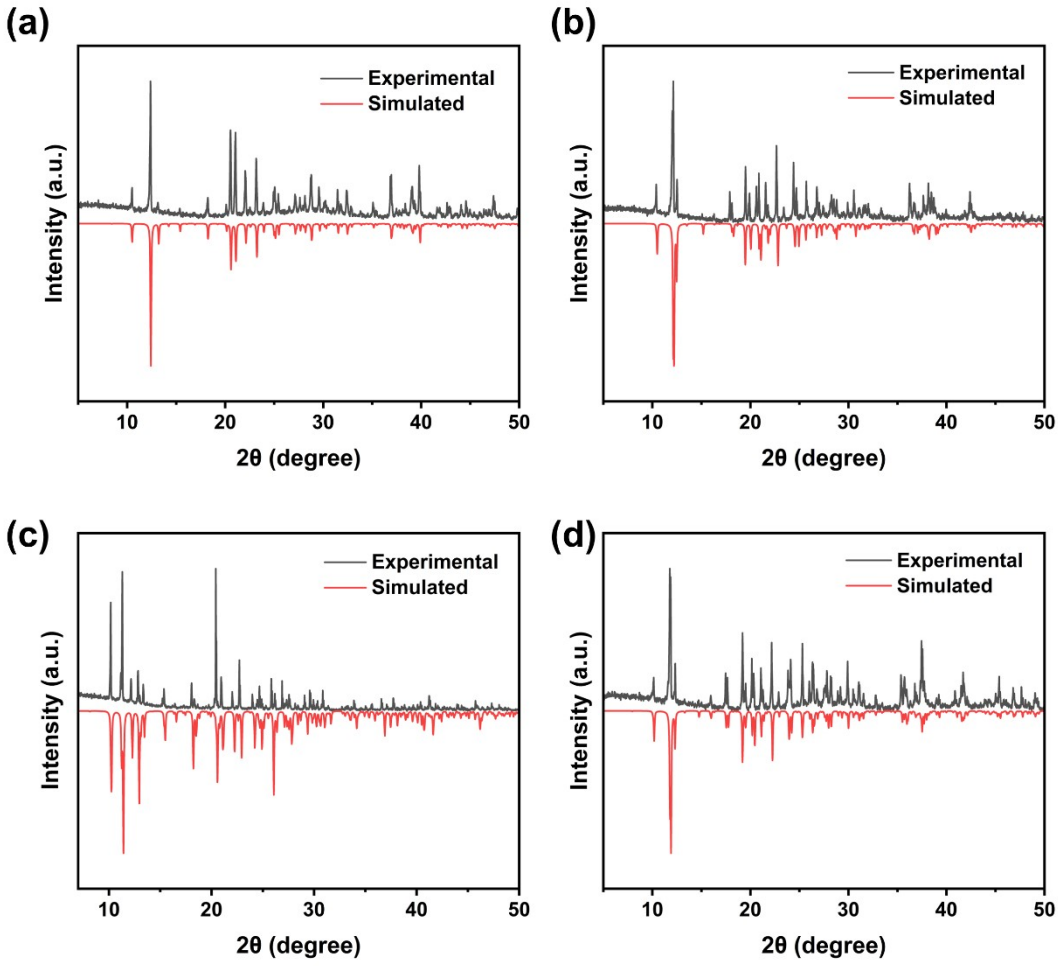

Fig. S7 Simulated and experimental PXRD patterns of compound **1** (a), **2** (b), **3** (c), and **4** (d) powders at room temperature.

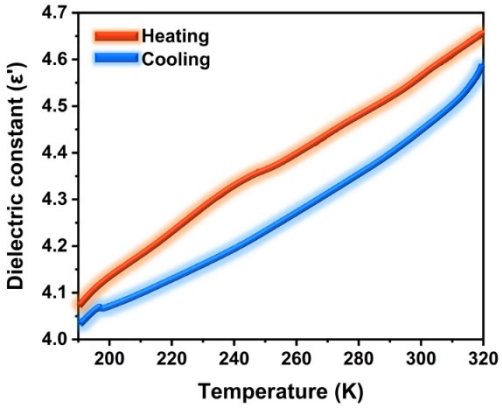

Fig. S8 Dielectric constant of **4** at 1 MHz.

Table S1 Chemical elemental analysis test results.

Compound	Calculated results			Experimental results		
1	C: 12.50	H: 3.12	N: 3.64	C: 12.27	H: 3.26	N: 3.85
2	C: 15.07	H: 3.52	N: 3.52	C: 14.63	H: 3.64	N: 3.71
3	C: 17.47	H: 3.88	N: 3.40	C: 17.14	H: 4.07	N: 3.53
4	C: 17.47	H: 3.88	N: 3.40	C:17.26	H: 3.98	N: 3.58

Table S2 Crystal data and structure refinement for Compounds **1**, **2**, and **3**.

Empirical formula	$(C_4H_{12}N)_2CdI_4$	$(C_4H_{12}N)_2CdI_4$	$(C_5H_{14}N)_2CdI_4$	$(C_5H_{14}N)_2CdI_4$	$(C_6H_{16}N)_2CdI_4$
Formula weight	768.29	768.29	796.34	796.34	824.39
Temperature	230 K	273 K	185 K	273 K	293 K
Crystal system	Monoclinic	Orthorhombic	Orthorhombic	Orthorhombic	Monoclinic
Space group	$P2_1/c$	*Pnma*	$P2_12_12_1$	*Pnma*	$P2_1/n$
a (Å)	13.3120 (5)	13.3771 (7)	9.5264 (2)	14.196 (7)	9.9568 (2)
b (Å)	9.6733 (3)	9.7035 (6)	14.3056 (4)	9.791 (5)	19.3258 (3)
c (Å)	33.4780 (12)	16.8488 (12)	16.5364 (4)	17.224 (10)	13.4592 (2)
α/°	90	90	90	90	90
β/°	90.115 (3)	90	90	90	100.675 (1)
γ/°	90	90	90	90	90
Z	8	4	4	4	4
Volume (Å^3)	4311.0 (3)	2187.1 (2)	2253.60 (10)	2394 (2)	2545.04 (8)
Dcalcd (mg m^{-3})	2.367	2.260	2.347	2.131	2.152
F (000)	2768	1288	1448	1336	1512
GOF	1.11	1.07	1.06	1.02	1.04

R_1 [I> 2σ(I)]	0.148	0.054	0.028	0.067	0.034
wR_2 [I> 2σ(I)]	0.348	0.166	0.071	0.284	0.093

Table S3 Crystal data and structure refinement for Compounds **4**.

Temperature	273 K
Empirical formula	$CdI_4 \cdot 2(C_6H_{16}N)$
Formula weight	824.39
Crystal system	Orthorhombic
Space group	*Pnma*
a (Å)	14.3623(6)
b (Å)	9.9781(6)
c (Å)	17.5752(8)
α/°	90
β/°	90
γ/°	90
Z	4
Volume ($Å^3$)	2518.7(2)
Dcalcd (mg m^{-3})	2.174
F (000)	1512
GOF	1.17
R_1 [I> 2σ(I)]	0.076
wR_2 [I> 2σ(I)]	0.248

Table S4 Selected bond lengths (Å) and bond angles for compound **1**.

230 K		273 K	
Bond	Bond lengths (Å)	Bond	Bond lengths (Å)
Cd1—I1	2.785 (4)	Cd1—I1	2.7677 (10)
Cd1—I2	2.760 (4)	Cd1—I1^{i}	2.7677 (10)
Cd1—I3	2.785 (4)	Cd1—I2	2.7731 (14)
Cd1—I4	2.771 (4)	Cd1—I3	2.7574 (15)
Cd2—I5	2.762 (4)		
Cd2—I6	2.781 (4)		
Cd2—I7	2.785 (4)		
Cd2—I8	2.771 (4)		
Bond angles	Angle (°)	Bond angles	Angle (°)
I1—Cd1—I3	108.16 (13)	I3—Cd1—I2	113.09 (5)
I4—Cd1—I3	109.01 (13)	I3—Cd1—I1^{i}	108.27 (4)
I4—Cd1—I1	110.00 (14)	I3—Cd1—I1	108.27 (4)
I2—Cd1—I3	112.18 (13)	I1^{i}—Cd1—I2	108.34 (3)
I2—Cd1—I1	109.16 (15)	I1—Cd1—I2	108.34 (3)
I2—Cd1—I4	108.32 (16)	I1—Cd1—I1^{i}	110.55 (6)

I6—Cd2—I7	109.14 (13)
I8—Cd2—I6	112.48 (13)
I8—Cd2—I7	109.15 (14)
I5—Cd2—I6	107.30 (13)
I5—Cd2—I8	107.88 (14)
I5—Cd2—I7	110.89 (14)

Symmetry codes: (i) x, $-y+3/2$, z; (ii) x, $-y+5/2$, z.

Table S5 Selected bond lengths (Å) and bond angles for compound **2**.

185 K		273 K	
Bond	Bond lengths (Å)	Bond	Bond lengths (Å)
Cd1—I1	2.7919 (7)	Cd00—I004	2.778 (9)
Cd1—I2	2.7759 (7)	Cd00—I004i	2.778 (9)
Cd1—I3	2.7853 (7)	Cd00—I2	2.761 (8)
Cd1—I4	2.7590 (7)	Cd00—I2i	2.761 (8)
		Cd00—I1i	2.774 (3)
		Cd00—I1	2.774 (3)
		Cd00—I4	2.764 (3)
		Cd00—I4i	2.764 (3)
Bond angles	Angle (°)	Bond	Angle (°)
I1—Cd1—I3	112.17 (2)	I004i—Cd00—I004	122.5 (3)
I4—Cd1—I3	106.35 (2)	I2—Cd00—I004	11.7 (3)
I4—Cd1—I1	109.32 (2)	I2i—Cd00—I004i	11.7 (2)
I2—Cd1—I3	109.79 (2)	I2—Cd00—I004i	111.98 (14)
I2—Cd1—I1	104.23 (2)	I2i—Cd00—I004	111.98 (14)
I2—Cd1—I4	115.13 (2)	I2—Cd00—I2i	101.0 (3)
		I2—Cd00—I1i	116.3 (3)
		I2—Cd00—I1	109.0 (3)
		I2i—Cd00—I1	116.3 (3)
		I2i—Cd00—I1i	109.0 (3)
		I2—Cd00—I4i	111.9 (3)
		I2i—Cd00—I4	111.9 (3)
		I2i—Cd00—I4i	104.5 (3)
		I2—Cd00—I4	104.5 (3)
		I1i—Cd00—I004i	99.4 (3)
		I1—Cd00—I004	99.4 (3)
		I1—Cd00—I004i	107.2 (3)
		I1i—Cd00—I004	107.2 (3)
		I1—Cd00—I1i	8.7 (4)
		I4i—Cd00—I004i	103.1 (3)
		I4—Cd00—I004i	111.5 (3)
		I4—Cd00—I004	103.1 (3)
		I4i—Cd00—I004	111.5 (3)
		I4i—Cd00—I1	113.49 (9)

	I4—Cd00—I1	112.74 (10)
	I4i—Cd00—I1i	112.74 (10)
	I4—Cd00—I1i	113.49 (9)
	I4i—Cd00—I4	9.1 (4)

Symmetry codes: (i) *x*, −*y*+1/2, *z*; (ii) *x*, −*y*+3/2, *z*.

Table S6 Selected bond lengths (Å) and bond angles for compound **3**.

293 K	
Bond	Bond lengths (Å)
Cd1—I1	2.7853 (5)
Cd1—I2	2.7557 (5)
Cd1—I3	2.7814 (5)
Cd1—I4	2.7571 (5)
Bond angles	Angle (°)
I1—Cd1—I3	107.947 (15)
I4—Cd1—I3	104.874 (18)
I4—Cd1—I1	112.638 (18)
I2—Cd1—I3	109.373 (16)
I2—Cd1—I1	107.600 (16)
I2—Cd1—I4	114.21 (2)

Table S7 Selected bond lengths (Å) and bond angles for compound **4**.

273 K	
Bond	Bond lengths (Å)
Cd1—I3	2.7642 (14)
Cd1—I1	2.7787 (16)
Cd1—I2i	2.7619 (12)
Cd1—I2	2.7619 (12)
Bond angles	Angle (°)
I3—Cd1—I1	114.02 (5)
I2i—Cd1—I3	108.32 (4)
I2—Cd1—I3	108.32 (4)
I2i—Cd1—I1	105.87 (4)
I2—Cd1—I1	105.87 (4)
I2i—Cd1—I2	114.60 (7)

Symmetry codes: (i) x, −y+3/2, z; (ii) x, −y+1/2, z.

Reference

1. M. Marino and K. Kreuer, Alkaline stability of quaternary ammonium cations for alkaline fuel cell membranes and ionic liquids, *Chemsuschem.*, 2015, **8**, 513-523.
2. Y.-Y. Luo, Z.-X. Zhang, C.-Y. Su, W.-Y. Zhang, P.-P. Shi, Q. Ye and D.-W. Fu, Tunable

optoelectronic response multifunctional materials: exploring switching and photoluminescence integrated in flexible thin films/crystals, *J. Mater. Chem. C.*, 2020, **8**, 7089-7095.